Development of an optimized synthetic Notch receptor as an in vivo cell–cell contact sensor

Li He[a], Jiuhong Huang[b], and Norbert Perrimon[a,c,1]

[a]Department of Genetics, Harvard Medical School, Boston, MA 02115; [b]School of Life Science and Technology, Tongji University, Shanghai 200092, China; and [c]Howard Hughes Medical Institute, Boston, MA 02115

Contributed by Norbert Perrimon, April 13, 2017 (sent for review February 24, 2017; reviewed by Christopher J. Potter and Koen Venken)

Detection and manipulation of direct cell–cell contact in complex tissues is a fundamental and challenging problem in many biological studies. Here, we report an optimized Notch-based synthetic receptor (synNQ) useful to study direct cell–cell interactions in *Drosophila*. With the synNQ system, cells expressing a synthetic receptor, which contains Notch activation machinery and a downstream transcriptional activator, QF, are activated by a synthetic GFP ligand expressed by contacting neighbor cells. To avoid *cis*-inhibition, mutually exclusive expression of the synthetic ligand and receptor is achieved using the "flippase-out" system. Expression of the synthetic GFP ligand is controlled by the Gal4/UAS system for easy and broad applications. Using synNQ, we successfully visualized cell–cell interactions within and between most fly tissues, revealing previously undocumented cell–cell contacts. Importantly, in addition to detection of cells in contact with one another, synNQ allows for genetic manipulation in all cells in contact with a targeted cell population, which we demonstrate in the context of cell competition in developing wing disks. Altogether, the synNQ genetic system will enable a broad range of studies of cell contact in developmental biology.

Notch | sensor | *Drosophila* | cell–cell contact

The ability of cells to interact with one another in multicellular organisms is central to almost all biological processes. Cells influence each other in two major ways: first, by indirect interaction through release of molecular signals into the free intracellular space, and, second, by direct interaction through physical cell–cell contacts, including the formation of junctions between mechanically coupled epithelial cells, synaptic connections between neurons, activation of lymphocytes by antigen-presenting cells, and infection of host cells by intracellular parasites. Malfunctions of direct cell–cell contact are associated with numerous diseases, including developmental defects, neurological disorders, immunological abnormalities, and cancers (1–3). Therefore, the ability to detect and manipulate cells that contact one another directly is fundamental to both basic and clinical research.

Detection of direct cell–cell contact can be challenging in complex tissues. Several methods have been used to address this problem, including different types of large-scale EM imaging, as well as labeling techniques (4, 5), GFP (green fluorescent protein) reconstitution across synaptic partners (GRASP) (6), HRP reconstitution (7), biotin labeling of intercellular contacts (8), and transsynaptic tracers (9). Although they are useful for specific applications, these approaches still suffer from several limitations, such as incompatibility with live cells, an inability to label and manipulate cells in contact simultaneously, artifactual effects on cell contact, or restriction to use in specific cell types.

To overcome these limitations and to visualize and manipulate direct cell–cell interactions effectively, we took a synthetic biology approach and engineered a genetic circuit that is activated by cell–cell contact. We focused on endogenous signaling mechanisms that require physical contact and found the highly conserved activity known as regulated intramembrane proteolysis (RIP) to be a suitable target for engineering. One of the best characterized RIP-dependent signaling molecules is Notch, a membrane receptor with a single transmembrane domain (10). Binding of a ligand to the extracellular domain of Notch induces proteolytic cleavage and release of its intracellular domain (ICD), which translocates to the nucleus and functions as a transcriptional factor (11) (Fig. 1 *A* and *B*). Notch signaling presents a number of advantages for engineering. First, the system is highly compact because it only involves a ligand and a receptor, together with several broadly expressed proteases (12). Second, unlike most other receptors, such as gated ion channels, G-protein–coupled receptors, and receptor tyrosine kinases, Notch is activated through mechanical forces generated by ligand–receptor binding (11, 13), such that the binding and activation machinery can be uncoupled to allow rewiring of the system with artificial interacting domains. Third, the ICD of Notch, which mediates downstream effects, can be replaced by other transcriptional factors without affecting its proteolytic activation (14, 15). We previously validated this approach in cultured *Drosophila* cells by replacing the ligand-binding domains of Notch with a GFP-binding nanobody, switching the ICD of Notch with the QF transcriptional activator, and activating this synthetic Notch receptor (synNQ) using a membrane-tethered artificial GFP ligand (16–18) (Fig. 1 *A* and *B*). More recently, similar synthetic Notch systems based on different artificial binding partners [i.e., mCD19, anti-mCD19 scFv (single-chain variable fragment)] were used to manipulate cell–cell communication in cultured mammalian cells, in the mouse immune system, and between fly neuron and glia cells (19–21).

Here, we further optimized our synNQ to develop an efficient genetic tool to study direct cell–cell contacts in vivo. We systematically tested the feasibility of synNQ to study cell interaction in various types of fly cells and tissues. Our results indicate that the synNQ system is highly robust and efficient in detecting cell–cell contact in different conditions and can be used effectively to manipulate gene expression in neighboring cells.

Significance

Direct cell–cell contacts are critical to diverse biological processes in multicellular organisms, including stem cell differentiation, tissue morphogenesis, neurotransmission, tumorigenesis, and immunological responses. However, identifying interacting cells in vivo is still a challenging task in complex tissues. Here, we introduce a new genetic tool, synthetic Notch receptor (synNQ), for efficient visualization and genetic manipulation of neighboring cells in vivo. This tool is functional in most fly tissues and can be easily applied using the widely adapted UAS/Gal4 system. Using both randomly generated clones and tissue-specific Gal4 lines, we demonstrate the applications of the synNQ system.

Author contributions: L.H. and J.H. designed research; L.H. and J.H. performed research; L.H., J.H., and N.P. analyzed data; and L.H., J.H., and N.P. wrote the paper.

Reviewers: C.J.P., Johns Hopkins University School of Medicine; and K.V., Baylor College of Medicine.

The authors declare no conflict of interest.

[1]To whom correspondence should be addressed. Email: perrimon@genetics.med.harvard.edu.

This article contains supporting information online at www.pnas.org/lookup/suppl/doi:10.1073/pnas.1703205114/-/DCSupplemental.

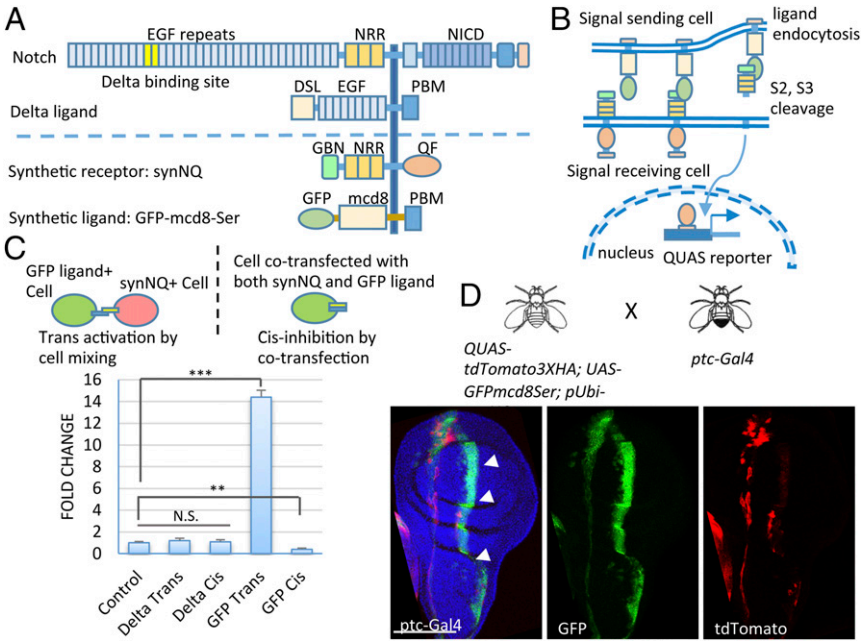

Fig. 1. Development of the synthetic cell–cell contact sensor in vitro and in vivo. (*A*) Schematic illustration of the *Drosophila* Notch receptor, Delta ligand, synNQ, and synthetic GFP ligand (GFP-mcd8-Ser). DSL, Delta/Serrate/Lag-2 motif; EGF, EGF-like repeats; GBN, GFP-binding nanobody; NICD, Notch intracellular domain; NRR, negative regulator region; PBM, PDZ-binding motif. (*B*) Activation of synNQ using GFP-mcd8-Ser. The artificial ligand and receptor first bind each other through GFP and GBN; then, the pulling force triggered by either cell movement or endocytosis triggers the conformational change of the NRR domain, and initiates the subsequent cleavage at the S2 and S3 sites to release the QF transcriptional factor into the cytosol. QF translocates into the nucleus to activate QUAS-controlled gene expression. (*C*) Testing of in vitro activation of synNQ using GFP-mcd8-Ser by mixing two cell populations expressing synNQ or ligand, respectively (transactivation), or cotransfection of both synNQ and ligand (*cis*-activation). Activity of synNQ was measured using a luciferase assay. The synNQ activity was not affected by native Delta ligand in either the *trans*-condition or *cis*-condition. GFP ligand significantly activated synNQ in the *trans*-condition and inhibited its activation in the *cis*-condition. The error bar indicates SEM. $^{**}P < 0.05$, $^{***}P < 0.01$. (*D*) synNQ was expressed ubiquitously in the fly wing disk. The *UAS-GFPmcd8Ser* ligand was driven by *ptc-Gal4*. Partial activation of synNQ (reported by *QUAS-tdTomato*) was detected in cells surrounding the GFP-positive cells. All blue channels are DAPI staining. N.S., not significant. (Scale bar: 100 μm.)

Results and Discussion

Development of an Optimized Synthetic Cell–Cell Contact Sensor for in Vitro and in Vivo Studies. In a previous report, we achieved a sixfold increase in receptor activation using a transprovided artificial GFP ligand (16). Using the same fly tissue culture system, we optimized the synNQ and ligand by incorporating different numbers of EGF repeats, testing Notch receptors from mouse and worm models, and manipulating endocytosis and dimerization of the ligand (Fig. S1). Combining both the optimized ligand and receptor, we were able to achieve a more than 14-fold increase in receptor activation (ratio between ligand-triggered activity and background activity without a ligand), as well as a threefold increase in absolute activity (the absolute activity of the receptors at a similar expression level) of the receptor (Fig. 1 *C* and *D* and Fig. S1). The optimized synNQ and GFP ligand are referred to as synNQ and GFPmcd8Ser, respectively.

Following in vitro optimization, we tested synNQ in vivo. Although synNQ does not interact with an endogenous ligand (Fig. 1*C*), the effect of overexpressing the synthetic receptor is unknown. Thus, we first tested the potential toxicity of synNQ using the fly heat shock (hs) promoter, which allowed us to control the expression time and level by shifting the temperature (22). Strong ubiquitous expression of synNQ can be induced after 1 h of hs at 37 °C (Fig. S2*A*). Ubiquitous expression of synNQ throughout developmental stages did not cause any detectable developmental defects or obvious abnormalities in adult flies, suggesting that synNQ is well tolerated in vivo. We also systematically tested the ligand-independent activity of synNQ in most larval and adult tissues, including the larval CNS (central nervous system), midgut, and imaginal disks and the adult brain, midgut, ovary, and testis. SynNQ is inactive in most of the tested tissues, with only a few specific cells constantly showing a detectable level of ligand-independent activation, which indicates potential machinery for noncanonical Notch activation in these cells (Fig. S2*B*). We also generated transgenic flies expressing synNQ ubiquitously using the *Drosophila Ubiquitin* promoter (pUbi), and found that these flies are viable and fertile without developmental phenotypes.

Next, we generated GFP ligand-positive cells using *ptc-Gal4*, *UAS-GFPmcd8Ser* at the anterior-posterior compartment boundary of the larval wing disk. Activation of synNQ was visualized through QUAS-controlled expression of the membrane-tethered mtdTomato. However, although the GFP ligand is strongly expressed using the UAS/Gal4 system (23), activation of synNQ in contacting cells was not very efficient (Fig. 1*D*), likely due to binding between synNQ and the GFP ligand in the same cell. Indeed, in cultured cells, expressing GFP ligand and synNQ in the same cell not only failed to activate the receptor but also significantly reduced background activity (Fig. 1*C*), suggesting that *cis*-provided synNQ interacts with the GFP ligand, thus reducing availability of the ligand. Similar *cis*-inhibition between a synNQ and a ligand has also been reported in mammalian tissue culture cells (19).

A previous study used different enhancers to drive the ligand and receptor in nonoverlapping domains (20). However, this approach is highly limited to available enhancers. To generate mutually exclusive expression of the ligand and receptor, we used the "FLP-out" strategy (24, 25), which uses flippase (FLP) recombinase-catalyzed excision of DNA sequences between tandemly oriented FLP recombination target (FRT) sites. We combined synNQ with a transcription stop signal, flanked it by FRT sequences, inserted the whole cassette before the GFP ligand, and put the entire construct under the control of the constitutive *Ubi* promoter (Fig. 2 *A* and *B*). In the absence of FLP recombinase, synNQ is expressed ubiquitously in all cells and expression of the GFP ligand is blocked. In

the presence of FLP, synNQ is excised, allowing the expression of the GFP ligand (Fig. 2*B*). We tested this system by expressing FLP using *UAS-FLP* and *ptc-Gal4*. Without *cis*-provided synNQ, GFP-positive cells triggered a very strong activation of synNQ in neighboring cells with 100% efficiency (Fig. 2 C–*E*), even though the expression level of the ligand induced by the *Ubi* promoter is weaker than the expression level of the ligand driven by the UAS/Gal4 system. This observation is consistent with the model that low-activation efficiency is indeed due to a *cis*-inhibition effect.

Activation of neighboring cells mainly occurred within a range of one to two cells, consistent with the idea that activation requires direct cell–cell contact (Fig. 2*E* and Fig. S3 *E* and *F*). In addition to activation in the neighboring disk epithelium, we observed strong synNQ activation in disk-associated myoblast cells (Fig. 2 *C* and *E*). This observation confirms the previously reported direct cell contact between myoblasts and disk epithelial cells (26). In addition, we detected a relatively weak but consistent activation of synNQ in squamous peripodial cells that lay over the GFP-positive columnar disk-proper cells (Fig. 2*E* and Fig. S4*A*). This observation is similar to a previous report that ectopic expression of Delta in peripodial cells triggers Notch activation in disk-proper cells (27), and provides further support that direct cell–cell contact occurs between the apical surfaces of these two distinct epithelial cell types. In addition, we noticed a clear enrichment of the GFP ligand in puncta associated with cytoneme-like cell protrusions (Fig. S3 *E* and *F*). Note that these puncta were not observed in the red channel (a membrane-tethered tdTomato through myristoylation), suggesting that they are not due to general membrane association (Fig. S3 *E* and *F*). Because the cytonemes are considered to be an important structure for morphogen movement and signaling (28), our observation suggests that the synNQ system does not affect endogenous signaling, and could be used to study signal transduction through cytonemes.

Because the FLP-out system can be used at all developmental stages, all cells derived from *ptc-Gal4*–positive cells are permanently labeled with the GFP ligand. Thus, our system can also be used as a lineage-tracing tool reminiscent of the previously reported G-trace system (29). Importantly, a *tubGal80ts* allele can be used to repress early Gal4 activity and achieve "real-time" capture of cell–cell interactions (Fig. 2*F*).

Test of SynNQ in Different Fly Organs Using Randomly Generated Ligand-Positive Cells. We further tested the induction of synNQ in adult and larval tissues by generating random GFP ligand-positive clones using hs-controlled *hs-FLP* (Fig. 3*A* and Fig. S3). In addition to disk epithelia (Fig. S3 *A*–*G*), activation of synNQ was observed in tracheal cells associated with gastric caeca (Fig. 3*B*), adult midgut progenitors in the larval midgut (Fig. 3*C*), salivary glands (Fig. 3*D*), lymph glands (Fig. 3*E*), follicle cells in the female ovary (Fig. 3 *F* and *G*), and adult midguts (Fig. S3*H*). Notably, when the entire germline of egg chambers expresses the GFP ligand, all of the follicle cells surrounding the germline (anterior and posterior follicle cells), or surrounded by germline cells [the migratory border cell (BC) cluster], showed synNQ activation (Fig. 3*G*).

One concern about the application of synNQ is that it introduces artificial binding between neighboring cells, which may affect normal biological process that require rapid changes in relative cell positions, such as cell migration. However, global induction of ligand-positive cells during early fly development (from the first-instar larval stage) does not cause any obvious lethality or developmental defects. Moreover, when the entire female germline expresses the GFP ligand, BCs migrate normally through the germline cells, remodeling of the centripetal follicle cell is unaffected, and posterior migration of the main body follicle cells is also unaffected (30) (Fig. 3*F*). The absence of detrimental effects is probably due to proteolytic activation of Notch, which removes the artificial bond after activation. This observation suggests that synNQ has advantages over other cell–cell contact visualization techniques, such as GRASP, that create a permanent artificial cell–cell bond (6).

Mapping Cell–Cell Contact Between Different Cell Types. Using different tissue-specific Gal4 lines, we detected activation of synNQ triggered by interactions between different cell types. For example, *btl-Gal4* triggers GFP-ligand expression specifically in tracheal cells (31). Expressing the ligand in the tracheal air sac strongly activated synNQ in the underlying myoblast cells and the disk epithelium

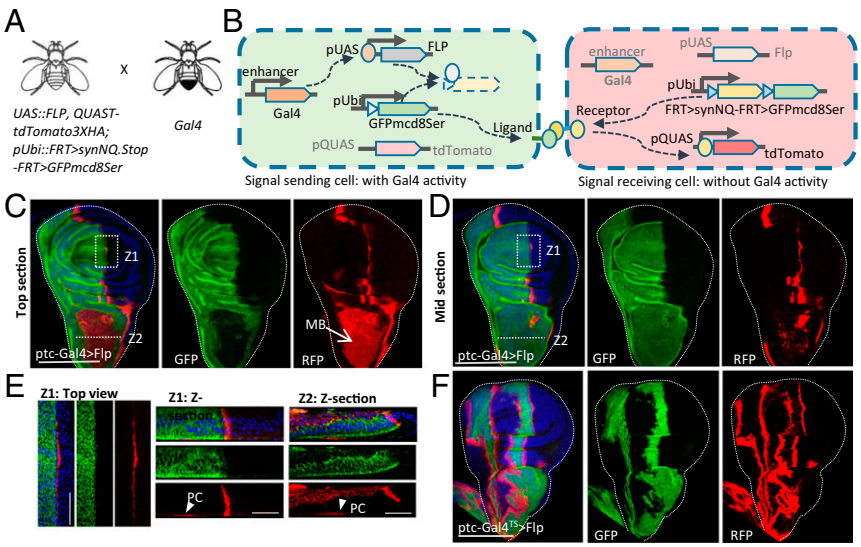

Fig. 2. Efficient activation of synNQ in neighboring cells using FLP-out strategy. (*A*) Genotype of flies to achieve mutual exclusive expression of GFP ligand and synNQ. (*B*) Schematic illustration of the synNQ FLP-out system using FLP driven by specific Gal4 lines. (*C*–*E*) Activation of the synNQ FLP-out system using *ptc-Gal4*. The whole disk was imaged in a series of z-sections, with the top and middle sections shown in *C* and *D*. Myoblast (MB) cells associated with the wing notum are indicated by a white arrow. The zoomed-in image and z-sections of zoom 1 and 2 (Z1 and Z2) are shown in *E*. synNQ activation in peripodial cells (PC) is indicated by arrowheads (Z1 and Z2 sections) (Fig. S4*A*). (*F*) Activation of synNQ using *Pct-Gal4* combined with *tubGal80^{TS}*. All blue channels are DAPI staining. (Scale bars: *C*, *D*, and *F*, 100 μm; *E*, 25 μm.)

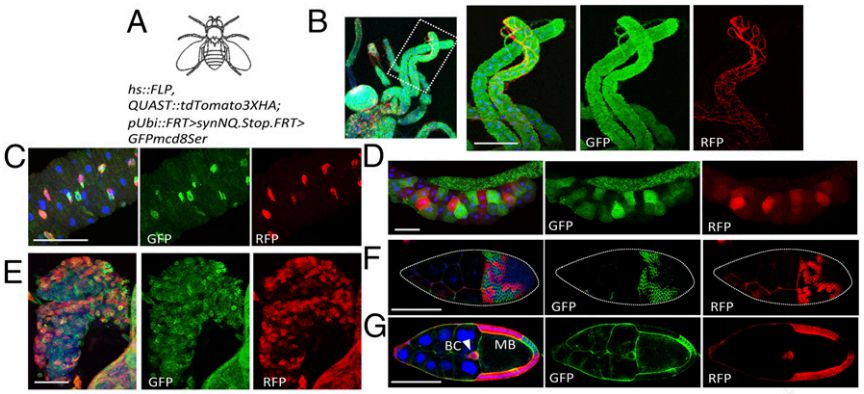

Fig. 3. Test of synNQ activation in neighboring cells through stochastically generated ligand-positive cells. (*A*) Genotype of flies used. (*B*) Activation of synNQ in tracheal cells surrounding the gastric cecum of the larval midgut. (*C*) Activation of synNQ in larval midgut adult midgut precursor cells. (*D*) Activation of synNQ in larval salivary glands. (*E*) Activation of synNQ in the larval lymph gland. (*F* and *G*) Activation of synNQ in adult female ovary follicle cells. Clones expressing GFP ligand efficiently activate synNQ in surrounding follicle cells in *F*. The germline (including both oocyte and nurse cells) expressing the GFP ligand activates all synNQ-expressing follicle cells surrounding them. A migratory BC cluster is highlighted by the arrowhead in *G*. MB, main body follicle cells. All blue channels are DAPI staining. (Scale bars: *B–D*, *F*, and *G*, 100 μm; *E*, 50 μm.)

(Fig. 4 *A* and *B*), consistent with previous reports of direct cell contact between these cell types (26, 32). This tracheal–myoblast interaction is confirmed by activation of synNQ in tracheal cells when the GFP ligand is expressed in myoblast cells with *dMef-Gal4* (Fig. S5 *A* and *B*). We also found that there are some fibroblast-like cells surrounding GFP-positive tracheal cells, a cell–cell contact that has not been reported before (Fig. 4*B*). These fibroblast-like cells, positioned on the top of tracheal cells, are dMef-positive, suggesting that they are also myoblast cells (Fig. S5*C*). Previously, myoblast cells have been reported to migrate proximally out of the wing disk notum to form the dorsal longitudinal indirect flight muscles (33). Our observation suggests that this migration may occur along the tracheal cells. In addition, we find that *blt-Gal4* labels larval brain motor neurons in the ventral nerve cord and activates the ensheathing glia cells (Fig. 4*C*). Further, the GFP ligand from tracheal cells specifically activates synNQ in proventricular ganglion cells in the larval midgut (34) (Fig. 4*D*), which is not activated by GFP ligands from midgut epithelial cells (Fig. S5*D*), suggesting that a special interaction exists between tracheal cells and particular neurons.

Interaction between glia and neurons in the larval brain was tested using the midline glia-specific *slit-Gal4* driver (35). The GFP ligand derived from Slit-positive cells strongly activated synNQ in specific neurons in the ventral ganglion (Fig. 4 *E* and *F*). *Slit-Gal4* also leads to strong ligand expression in the fly prothoracic gland and activated synNQ in the corpus allatum. Importantly, consistent with previous results (36), neurons that send axons into the ring gland can be clearly visualized after a longer exposure (Fig. 4*G*). These data, together with previous observations made using a trachea-specific Gal4 (Fig. 4*D*), suggest that synNQ is an efficient tool for identification of neurons that target an organ of interest.

We also tested whether synNQ can detect interactions between hemocytes and other larval tissues using *Hermese-Gal4* (*He-Gal4*), a commonly used pan-hemocyte marker expressed in both undifferentiated and differentiated larval hemocytes (37–39).

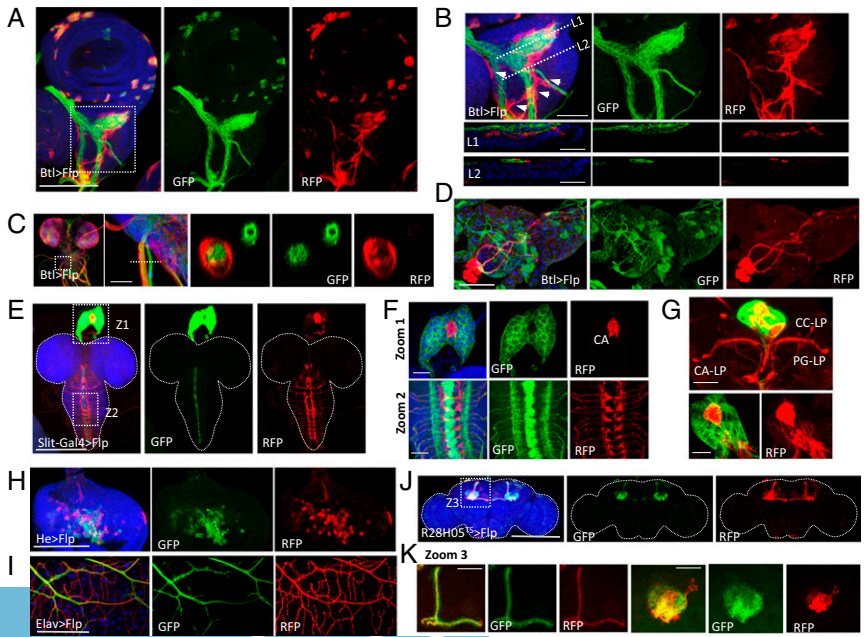

Fig. 4. Activation of synNQ in neighboring cells using tissue-specific Gal4 drivers. Activation of synNQ using tracheal-specific *Btl-Gal4* in the wing disk (*A* and *B*), larval brain (*C*), and larval midgut (*D*). In *B*, tracheal associated fibroblast-like cells are indicated by the arrowheads, and L1 and L2 are cross-sections of the sample at the indicated position using the dashed line. (*E–G*) Activation of synNQ using *slit-Gal4* in the larval brain ventral nerve cord and ring gland. CA, corpus allatum. CA-LP, corpus allatum innervating neurosecretory neurons of the lateral protocerebrum; CC-LP, corpora cardiaca innervating neurosecretory neurons of the lateral protocerebrum; PG-LP, prothoracic gland innervating neurosecretory neurons of the lateral protocerebrum. (*H*) SynNQ activity in eye disk-associated hemocytes labeled by *He-Gal4*. (*I*) SynNQ activation in motor neurons associated with the male accessory gland using *Elav-Gal4*. (*J* and *K*) Activation of synNQ controlled by a mushroom body-specific Gal4 in the adult brain. The indicated white rectangular region is enlarged in *K*. All blue channels are DAPI staining. (Scale bars: *A*, *D*, *E*, *H*, *I*, and *J*, 100 μm; *B*, 25 μm; *C*, 10 μm; *F*, *G*, and *K*, 20 μm.)

However, no clear synNQ activation was detected in the larval organs examined, including the brain, disk epithelium, and midgut. Interestingly, however, synNQ was activated in a special group of cells with hemocyte-like morphology that associate with the posterior region of the eye imaginal disk (40) (Fig. 4*H*). We checked whether these cells correspond to migratory glia also located at the posterior region of the eye disk. However, they were negative for the glia-specific marker Repo (Fig. S6*A*). One possible explanation is that the FLP-out system fails to label all of the hemocytes that are expressing *He-Gal4* efficiently; therefore, the observed synNQ-active red cells may still be regular hemocytes positive for He. To test this possibility, we used *He-Gal4* combined with *UAS-nlsGFP* to activate synNQ. If the observation is due to inefficient labeling, synNQ-active cells should also be positive for nlsGFP. Strikingly, synNQ-positive cells were negative for nlsGFP (Fig. S6 *B* and *C*). In addition, synNQ triggered by another classic pan-hemocyte marker, *HmlΔ-Gal4*, combined with *UAS-nlsGFP* also revealed similar unlabeled cell populations (Fig. S6*D*). These data suggest that there may be a previously unidentified population of hemocytes that are not derived from He- or Hml-positive cells.

Another unexpected synNQ activation was observed with *Elav-Gal4*, which is thought to label all neurons (23). *Elav-Gal4* triggers GFP expression in larval CNS and motor neurons, and activates synNQ in the associated glia cells (Fig. S7 *A* and *B*). Surprisingly, in the adult male reproductive organ, ensheathing glia cells surrounding the motor neurons are positive for GFP ligand, and strong activation of synNQ in the motor neurons was observed (Fig. 4*I* and Fig. S6). Labeling of glial cells is expected because Elav is transiently expressed in glia cells during differentiation (41). However, the absence of GFP ligand in motor neurons suggests that *Elav-Gal4* may not label all neuronal lineages.

Finally, we tested the ability of the synNQ system to map long-distance connections between neurons. Using *R28H05-Gal4*, which specifically labels neurons of the mushroom body in the adult brain (42), we observed activation of synNQ within the same neuron cluster (in this experiment, the *FRT > synNQ.Stop.FRT > GFPmcd8Ser* was controlled by the *Elav* promoter to avoid activation of synNQ in glia cells) (Fig. 4 *J* and *K*). However, no clear axon extending in or out of the mushroom body was observed. We also tested whether the synNQ system can be used to detect interneuron connections through a single axon by testing the ability of the system to detect the connection between olfactory-receptor neurons (ORNs) and neurons in the antennal lobe. Expressing the GFP ligand in ORNs using *Gr21a-Gal4* did not trigger any detectable activation of synNQ in the adult brain (Fig. S8*B*). Previously, in a mammalian tissue system, a similar synNQ detected cell interactions in cocultured primary neurons and leukemia cells; however, in that case, a considerably larger contact surface was formed between the cells (19).

The current synNQ system is effective in mapping cell–cell contacts between most types of cells. However, mapping special types of cell–cell contacts still requires specific engineering. Such contacts include transient interactions, such as interactions between hemocytes and other tissues, and stable interactions with a highly limited interaction surface, such as neurons that are connected through few synapses. In such applications, all current synthetic Notch systems have the same caveat; that is, they respond to the trigger linearly, with the amount of activated receptor, and thus released transcriptional factor, generally proportional to the contacting surface area and the duration of this contact. A stable contact (several hours) and a large cell–cell contact surface (~10–20 μm^2) between epithelial cells will generate significantly stronger signal than an unstable contact (several minutes) and/or a small interacting surface (<1 μm^2 for a typical synapse). One strategy to overcome the weak signal issue is to increase the concentration of the ligand and receptor at the contact location, which should have an effect equal to the effect of an increase in the functional contact surface. Therefore, one solution is to increase the expression level of the ligand and the receptor using a stronger binary expression system and to target the ligand and receptor to a specific area of interest, such as a synapse. Another solution would be to use a nonlinear response system as a readout, such as a binary switch system like FLP/FRT or a similar system.

Manipulation of Neighboring Cells to Study Cell–Cell Competition in Developing Epithelia. Cell competition is a contact-dependent cell–cell interaction mechanism that eliminates slowly dividing cells or damaged cells with tumorigenesis potential, a mechanism that can sometimes be hijacked by tumor cells to expand at the expense of wild-type (WT) neighbors (43, 44) (Fig. 5*A*). To test the effectiveness of synNQ for genetic manipulation of neighboring cells, we used synNQ to control the expression of *QUAS-Lgl^{RNAi}*, which knocks down the cell polarity gene lethal giant larvae (*Lgl*) (Fig. 5*A*). Cells with reduced *Lgl* are eliminated through cell competition (45). Interestingly, after induction of random clones in the wing disk, knocking down *Lgl* in cells surrounding the GFP-positive clones causes a significant reduction in both synNQ-active cells (red cells labeled by mtdTomato) and the surrounding WT GFP-positive cells (Fig. 5 *B* and *C*). The elimination of GFP-positive WT cells may be caused by sustained activation of JNK in WT cells during the cell competition process or by the destabilization of the cell–cell boundary caused by apoptosis of neighboring cells (46).

Concluding Remarks. We report the optimization of a genetic tool, the synNQ system, and its effectiveness in vivo. Our results showed that synNQ is an efficient method to label and manipulate cells in contact with one another in various cell types and tissues, including flat epithelial cells, neurons, glia, hemocytes, myoblasts, and tubular tracheal cells. The synNQ system combines user-friendly

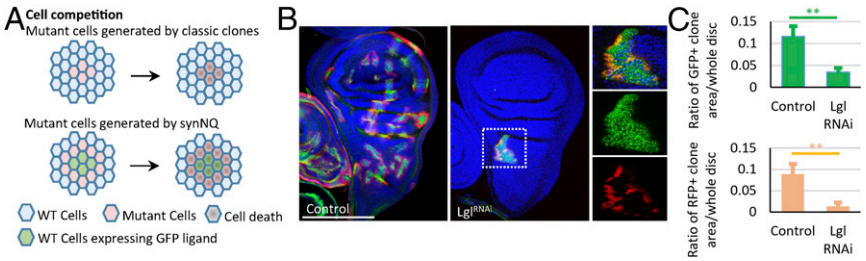

Fig. 5. Manipulation of contacting cells using the synNQ system. (*A*) Cell competition happens between mutant cells (pink) and WT cells (blue). (*Top*) Previous reports have shown that mutant cells are eliminated by a WT neighbor. (*Bottom*) Here, mutant cells are created in the surrounding cells around a WT clone. (*B*) SynNQ was activated in cells surrounding the GFP-positive clone in control tissue. Knocking down *Lgl* in cells surrounding the GFP-positive clones with *QUAS-Lgl^{RNAi}* eliminates not only the mutant cells but also the WT GFP-positive cells. Imaginal disks were tested after 5-d hs induction of clones. All blue channels are DAPI staining. (Scale bar: 100 μm.) (*C*) Quantification of GFP-positive and RFP-positive cell areas compared with the total wing disk area. The error bar indicates SEM. $^{**}P < 0.05$.

genetics for direct application with a single cross to any Gal4 lines of interest. In addition, using the tubGal80 temperature-sensitive system, precise spatiotemporal control of the synNQ can be easily achieved. When the QF transcriptional factor is used as the downstream effector, its effects can also be inhibited by the QF-specific inhibitor QS and derepressed by quinic acid, thus providing another layer of flexibility to the system (17). Finally, the QF transcriptional factor of synNQ could be replaced with different flavors of Cas9 to either change the target gene (generation of targeted mutation) permanently or manipulate endogenous gene expression (CRISPRi or CRISPRa) (47).

The synNQ system is a robust tool for developmental biology studies. For example, we identified cell–cell interactions between tracheal cells and neurons, unreported cells associated with hemocytes, and a potential new origin of motor neurons. These observations greatly benefit from the ability of synNQ to highlight contacting cells functionally in a way that no previous genetic tool has achieved.

We anticipate that synNQ will be generally useful for many studies, including study of cell–cell interactions in tumor invasion; detection of GFP-tagged proteins immobilized in the extracellular space, such as extracellular matrix (ECM) protein or secreted factors associated with ECM; or imaging cell–cell interactions in real-time using live-cell imaging. We also expect that future engineering of better ligand and receptor pairs with low background activity and high induced responses, as well as using different protein-targeting strategies or alternative signal readouts, will make synthetic Notch systems useful for a much broader range of applications.

Materials and Methods

All DNA constructs were verified by sequencing. Sequences of cDNAs and plasmids can be found in Dataset S1 Transgenic flies were generated by BestGene, Inc. Flies were reared on standard cornmeal/agar medium supplemented with yeast. Adult flies were entrained in 12:12 light/dark cycles at 25 °C. For the FLP-out experiments, first-instar larvae or young adults (3–5 d after eclosion) were heat-shocked at 37 °C for 0.5 h. Additional information about the experimental methods and full genotypes of each figure can be found in *SI Materials and Methods*.

ACKNOWLEDGMENTS. We thank Dr. Ginger L. Hunter, Dr. Stephen C. Blacklow, Dr. Xiang Ma, and Dr. Qinghua Zhou for support and advice and Stephanie Mohr, Ben Ewen-Campen, and Justin Bosch for comments on the manuscript. This work was supported by the Damon Runyon Cancer Research Foundation (L.H.) and NIH Grant R21DA039582. J.H. is funded by the China Scholarship Council (CSC) (Award 201306260106). N.P. is an investigator of the Howard Hughes Medical Institute.

1. Kamińska K, et al. (2015) The role of the cell-cell interactions in cancer progression. *J Cell Mol Med* 19:283–296.
2. Akins MR, Biederer T (2006) Cell-cell interactions in synaptogenesis. *Curr Opin Neurobiol* 16:83–89.
3. Mammoto T, Ingber DE (2010) Mechanical control of tissue and organ development. *Development* 137:1407–1420.
4. Rah JC, Feng L, Druckmann S, Lee H, Kim J (2015) From a meso- to micro-scale connectome: Array tomography and mGRASP. *Front Neuroanat* 9:78.
5. Cazemier JL, Clascá F, Tiesinga PH (2016) Connectomic analysis of brain networks: Novel techniques and future directions. *Front Neuroanat* 10:110.
6. Feinberg EH, et al. (2008) GFP Reconstitution Across Synaptic Partners (GRASP) defines cell contacts and synapses in living nervous systems. *Neuron* 57:353–363.
7. Martell JD, et al. (2016) A split horseradish peroxidase for the detection of intercellular protein-protein interactions and sensitive visualization of synapses. *Nat Biotechnol* 34: 774–780.
8. Desbois M, Cook SJ, Emmons SW, Bülow HE (2015) Directional trans-synaptic labeling of specific neuronal connections in live animals. *Genetics* 200:697–705.
9. Wickersham IR, Finke S, Conzelmann KK, Callaway EM (2007) Retrograde neuronal tracing with a deletion-mutant rabies virus. *Nat Methods* 4:47–49.
10. Lal M, Caplan M (2011) Regulated intramembrane proteolysis: Signaling pathways and biological functions. *Physiology (Bethesda)* 26:34–44.
11. Chillakuri CR, Sheppard D, Lea SM, Handford PA (2012) Notch receptor-ligand binding and activation: Insights from molecular studies. *Semin Cell Dev Biol* 23:421–428.
12. Hébert SS, et al. (2004) Coordinated and widespread expression of gamma-secretase in vivo: Evidence for size and molecular heterogeneity. *Neurobiol Dis* 17:260–272.
13. Gordon WR, et al. (2007) Structural basis for autoinhibition of Notch. *Nat Struct Mol Biol* 14:295–300.
14. Struhl G, Adachi A (1998) Nuclear access and action of notch in vivo. *Cell* 93:649–660.
15. Lieber T, Kidd S, Struhl G (2011) DSL-Notch signaling in the Drosophila brain in response to olfactory stimulation. *Neuron* 69:468–481.
16. Gordon WR, et al. (2015) Mechanical allostery: Evidence for a force requirement in the proteolytic activation of Notch. *Dev Cell* 33:729–736.
17. Potter CJ, Tasic B, Russler EV, Liang L, Luo L (2010) The Q system: A repressible binary system for transgene expression, lineage tracing, and mosaic analysis. *Cell* 141:536–548.
18. Rothbauer U, et al. (2006) Targeting and tracing antigens in live cells with fluorescent nanobodies. *Nat Methods* 3:887–889.
19. Morsut L, et al. (2016) Engineering customized cell sensing and response behaviors using synthetic Notch receptors. *Cell* 164:780–791.
20. Huang TH, Velho T, Lois C (2016) Monitoring cell-cell contacts in vivo in transgenic animals. *Development* 143:4073–4084.
21. Roybal KT, et al. (2016) Engineering T cells with customized therapeutic response programs using synthetic Notch receptors. *Cell* 167:419.e16–432.e16.
22. Pelham HR (1982) A regulatory upstream promoter element in the Drosophila hsp 70 heat-shock gene. *Cell* 30:517–528.
23. Brand AH, Perrimon N (1993) Targeted gene expression as a means of altering cell fates and generating dominant phenotypes. *Development* 118:401–415.
24. Harrison DA, Perrimon N (1993) Simple and efficient generation of marked clones in Drosophila. *Curr Biol* 3:424–433.
25. Golic KG, Lindquist S (1989) The FLP recombinase of yeast catalyzes site-specific recombination in the Drosophila genome. *Cell* 59:499–509.
26. Huang H, Kornberg TB (2015) Myoblast cytonemes mediate Wg signaling from the wing imaginal disc and Delta-Notch signaling to the air sac primordium. *eLife* 4:e06114.
27. Pallavi SK, Shashidhara LS (2005) Signaling interactions between squamous and columnar epithelia of the Drosophila wing disc. *J Cell Sci* 118:3363–3370.
28. Kornberg TB (2014) Cytonemes and the dispersion of morphogens. *Wiley Interdiscip Rev Dev Biol* 3:445–463.
29. Evans CJ, et al. (2009) G-TRACE: Rapid Gal4-based cell lineage analysis in Drosophila. *Nat Methods* 6:603–605.
30. Horne-Badovinac S, Bilder D (2005) Mass transit: Epithelial morphogenesis in the Drosophila egg chamber. *Dev Dyn* 232:559–574.
31. Shiga Y, Tanaka-Matakatsu M, Hayashi S (1996) A nuclear GFP/ beta-galactosidase fusion protein as a marker for morphogenesis in living *Drosophila*. *Dev Growth Differ* 38:99–106.
32. Roy S, Hsiung F, Kornberg TB (2011) Specificity of Drosophila cytonemes for distinct signaling pathways. *Science* 332:354–358.
33. Roy S, VijayRaghavan K (1997) Homeotic genes and the regulation of myoblast migration, fusion, and fibre-specific gene expression during adult myogenesis in Drosophila. *Development* 124:3333–3341.
34. Schoofs A, Hückesfeld S, Surendran S, Pankratz MJ (2014) Serotonergic pathways in the Drosophila larval enteric nervous system. *J Insect Physiol* 69:118–125.
35. Scholz H, Sadlowski E, Klaes A, Klämbt C (1997) Control of midline glia development in the embryonic Drosophila CNS. *Mech Dev* 64:137–151.
36. Siegmund T, Korge G (2001) Innervation of the ring gland of Drosophila melanogaster. *J Comp Neurol* 431:481–491.
37. Zettervall CJ, et al. (2004) A directed screen for genes involved in Drosophila blood cell activation. *Proc Natl Acad Sci USA* 101:14192–14197.
38. Evans CJ, Liu T, Banerjee U (2014) Drosophila hematopoiesis: Markers and methods for molecular genetic analysis. *Methods* 68:242–251.
39. Jung SH, Evans CJ, Uemura C, Banerjee U (2005) The Drosophila lymph gland as a developmental model of hematopoiesis. *Development* 132:2521–2533.
40. Froldi F, et al. (2010) The lethal giant larvae tumour suppressor mutation requires dMyc oncoprotein to promote clonal malignancy. *BMC Biol* 8:33.
41. Berger C, Renner S, Lüer K, Technau GM (2007) The commonly used marker ELAV is transiently expressed in neuroblasts and glial cells in the Drosophila embryonic CNS. *Dev Dyn* 236:3562–3568.
42. Li HH, et al. (2014) A GAL4 driver resource for developmental and behavioral studies on the larval CNS of Drosophila. *Cell Reports* 8:897–908.
43. Merino MM, Levayer R, Moreno E (2016) Survival of the Fittest: Essential roles of cell competition in development, aging, and cancer. *Trends Cell Biol* 26:776–788.
44. Di Gregorio A, Bowling S, Rodriguez TA (2016) Cell competition and its role in the regulation of cell fitness from development to cancer. *Dev Cell* 38:621–634.
45. Menéndez J, Pérez-Garijo A, Calleja M, Morata G (2010) A tumor-suppressing mechanism in Drosophila involving cell competition and the Hippo pathway. *Proc Natl Acad Sci USA* 107:14651–14656.
46. Tamori Y, Deng WM (2011) Cell competition and its implications for development and cancer. *J Genet Genom* 38:483–495.
47. Dominguez AA, Lim WA, Qi LS (2016) Beyond editing: Repurposing CRISPR-Cas9 for precision genome regulation and interrogation. *Nat Rev Mol Cell Biol* 17:5–15.
48. Riabinina O, et al. (2015) Improved and expanded Q-system reagents for genetic manipulations. *Nat Methods* 12:219–222.
49. Ni JQ, et al. (2008) Vector and parameters for targeted transgenic RNA interference in Drosophila melanogaster. *Nat Methods* 5:49–51.
50. Spriestersbach A, Kubicek J, Schäfer F, Block H, Maertens B (2015) Purification of His-tagged proteins. *Methods Enzymol* 559:1–15.